

# Aerial Vision-and-Language Navigation via Semantic-Topo-Metric Representation Guided LLM Reasoning

Yunpeng Gao<sup>1,2\*</sup>, Zhigang Wang<sup>2\*</sup>, Linglin Jing<sup>2</sup>, Dong Wang<sup>2</sup>, Xuelong Li<sup>2,3</sup>, Bin Zhao<sup>1,2†</sup>

**Abstract**—Aerial Vision-and-Language Navigation (VLN) is a novel task enabling Unmanned Aerial Vehicles (UAVs) to navigate in outdoor environments through natural language instructions and visual cues. It remains challenging due to the complex spatial relationships in outdoor aerial scenes. In this paper, we propose an end-to-end zero-shot framework for aerial VLN tasks, where the large language model (LLM) is introduced as our agent for action prediction. Specifically, we develop a novel Semantic-Topo-Metric Representation (STMR) to enhance the spatial reasoning ability of LLMs. This is achieved by extracting and projecting instruction-related semantic masks of landmarks into a top-down map that contains the location information of surrounding landmarks. Further, this map is transformed into a matrix representation with distance metrics as the text prompt to the LLM, for action prediction according to the instruction. Experiments conducted in real and simulation environments have successfully proved the effectiveness and robustness of our method, achieving 15.9% and 12.5% improvements (absolute) in Oracle Success Rate (OSR) on AerialVNL-S dataset.

## I. INTRODUCTION

The Aerial Vision-and-Language Navigation (Aerial VLN) [1] emerges as a groundbreaking task. It enables unmanned aerial vehicles (UAVs) to interpret natural language instructions and corresponding visual information to navigate in outdoor environments. This technology can eliminate the necessity for manual UAV operation by human pilots, clearly mitigating the barriers to human-UAV interaction and potentially benefitting search, rescue, and delivery tasks.

Recently, VLN tasks have been well-developed. Considering the powerful reasoning capability of large language models (LLMs) [2], [3], [4], [5], several VLN methods have started to use LLMs as agents to parse instructions and predict actions [6], [7], [8], [9]. Specifically, existing methods attempt to describe the visual observations with text to enhance the LLM’s scene understanding ability. NavGPT [6] converted visual scene semantics into text description for the LLM to conduct high-level planning. MapGPT [10] introduced a topological graph described in language as text prompts to an LLM, guiding low-level planners to explore new nodes of a predefined graph of the environment.

Although existing VLN methods have made significant progress, most of them are designed for indoor or ground-based outdoor environments and pay less attention to aerial

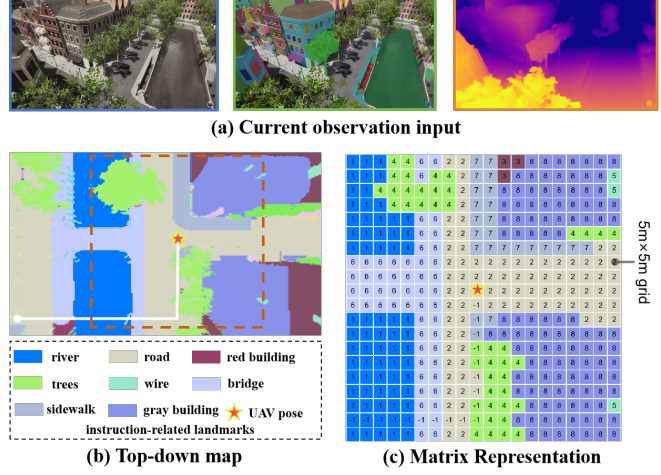


Fig. 1: The pipeline to obtain STMR. Observation image, semantic mask, and depth image (a) will be aggregated in the top-down map (red dashed box) (b), which captures the Semantic-Topo-Metric information of the neighborhood of the current position, further generating a 20x20 matrix representation (c).

VLN tasks. Practically, the rich semantics, complex spatial relationships, and the large-scale nature of outdoor 3D spaces make it challenging for existing VLN methods to adapt to aerial scenarios. As shown in Fig. 1 (a), the aerial scene can be quite complex, which may lead to incorrect reasoning for several reasons, such as an overemphasis on instruction-irrelevant objects, or a failure to capture the contextual relationships between different areas. Furthermore, the vast scale of aerial landscapes can further complicate navigation, making local-perspective-based VLN methods unable to comprehend the environment. Thus, the development of VLN methods that integrate both effective semantic information and precise spatial representations is urgently needed to enhance the adaptability and accuracy in aerial scenarios.

To overcome these challenges, we propose a zero-shot LLM-based aerial VLN framework, which takes natural language instructions, RGB images, and depth images as input, and directly makes action predictions (*e.g.*, forward 10 meters) through single-step reasoning updates. Specifically, a Semantic-Topo-Metric Representation (STMR) is designed for LLMs prompting. We first extract instruction-related landmarks and obtain corresponding semantic masks by perception models, *i.e.*, Grounding Dino [11] and Tokenize Anything [12]. After that, semantic masks obtained from each step are gradually projected into a top-down map using

\*Equal Contribution, †Corresponding Author

<sup>1</sup>Northwestern Polytechnical University

<sup>2</sup>Shanghai AI Laboratory

<sup>3</sup>Institute of Artificial Intelligence, China Telecom Corp Ltd

depth and pose transformation as shown in [Fig. 1](#) (b). This projected map encompasses both the UAV’s travel trajectory and spatial information, *i.e.*, locations of surrounding objects. To integrate rich visual information and topology into the text prompt while maintaining its simplicity, we separate the top-down map centered at the UAV’s current position into grids and substitute each grid with a semantic number. This process transforms the top-down map into a matrix representation, tailored to serve as a spatial prompt for the LLM. As can be seen from [Fig. 1](#) (c), the matrix representation encompasses topological, semantic, and metric information, and is input to an LLM together with historical actions, sub-goal instructions, and other information to infer the next action. Compared with other learning-based and LLM-based methods, the proposed method effectively improves the accuracy of spatial reasoning.

Our contributions are summarized as follows:

- To our knowledge, we propose the first LLM-based end-to-end framework for the aerial VLN task, facilitating the development of UAV navigators. This framework requires no training and no extra low-level action planner, thus allowing for easy integration.
- We propose the Semantic-Topo-Metric Representation (STMR), a unique matrix representation that encompasses topological, semantic, and metric information. STMR is designed to significantly enhance the spatial-aware reasoning capabilities of LLMs in outdoor environments.
- Extensive experiments on the aerial VLN task especially in real environments demonstrate that the proposed method outperforms previous state-of-the-art methods by a large margin, establishing a strong baseline for future zero-shot Aerial VLN tasks.

## II. RELATED WORK

*a) Vision-Language Navigation (VLN):* VLN aims to enable autonomous agents to navigate complex environments by understanding and executing natural language instructions based on visual context. Early VLN methods use sequence-to-sequence LSTMs to predict low-level actions [13] or high-level actions from panoramas [14]. Several attention processes have been proposed [15], [16], [17] to enhance the process of learning visual textual correspondence. Reinforcement learning is also explored to improve policy learning [18], [19], [20]. Besides, transformer-based architecture have shown superior performance to long-distance contextual information [21], [22]. More recent works [6], [10] leverage the reasoning and dialogue capabilities of LLMs, achieving great progress. However, most of them are developed under a ground-based, discrete VLN setting, which simplifies navigation as traversing on a predefined graph on the ground. This limits the free movement space of UAVs in the real world. Aerial VLN remains challenging due to the large-scale and complex environments.

*b) UAV navigation:* Unmanned Aerial Vehicle (UAV) navigation has seen a surge of interest over the past few decades. Guided with instructions, Blukis *et al.* [23] use imitation learning for low-level velocity command prediction. [24] predicts interpretable position-visitation distributions to guide UAV’s control actions, using a combination of supervised and imitation learning for efficient training. Misra *et al.* [25] decompose instruction execution in two stages, separately using supervised learning for goal prediction and policy gradient for action generation. AerialVNL [1] contributes a much more challenging aerial VLN dataset focusing on large-scale environments, and provides a look-ahead guidance method as the baseline. Despite the progress, the generalizability and performance of these methods still require improvement.

*c) LLMs for robot planning and interaction:* Most recently, LLMs have demonstrated impressive capabilities in understanding and reasoning. To leverage these capabilities, several promising methods have been proposed for applying LLMs in robotic systems. A few methods involve using LLM-generated rewards optimized in simulation to improve control [26], [27]. Others utilize LLM-selected subgoals as an abstraction to enhance policies for navigation [28], [29] and manipulation [30], [31]. Additionally, research has explored the use of LLMs to generate executable code for control and perception primitives [32], [33], [34]. Despite their potential, LLMs are still prone to confidently hallucinating outputs, such as referring to objects not observed in the scene [35]. In order to alleviate the hallucinating phenomenon, we propose a matrix-based representation containing topological, semantic, and metric information for better prompting the LLMs.

## III. METHOD

In this paper, we introduce a novel zero-shot framework that leverages large language models (LLMs) for action prediction in aerial VLN tasks. As shown in [Fig. 2](#), our framework mainly consists of three modules. The sub-goal extracting module decomposes language instructions into several sub-goals, facilitating step-by-step reasoning and navigation. The Semantic-Topo-Metric Representation (STMR) module represents the outdoor environment as a matrix containing semantic, topological, and metric information for the prompt to an LLM. Finally, the LLM planner outputs its current thoughts and actions by using the prompts from the aforementioned two modules along with the task description and history as inputs.

### A. Problem Formulation

In an aerial VLN task, the problem is formulated as a free-form language instruction guided navigation. At the beginning of each episode, the UAV is placed in an initial pose  $P = [x, y, z, \phi, \theta, \psi]$ , where  $(x, y, z)$  denotes the UAV’s position and  $(\phi, \theta, \psi)$  represents pitch, roll, and yaw of the UAV’s orientation. A natural language instruction  $L$  is

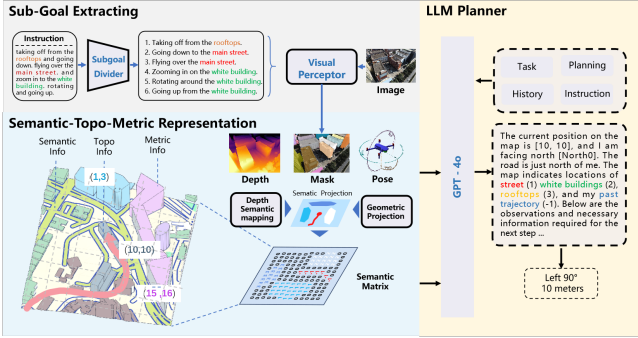


Fig. 2: Our method consists of three modules, *i.e.* sub-goal extracting, Semantic-Topo-Metric Representing, and LLM planner. First, we prompt an LLM to break down long instructions and extract specific landmarks, which will be classified by perception models, generating corresponding semantic masks. Then we project these masks into a top-down map using the UAV-view pose and depth information. The map is further compressed into a matrix representation. Finally, we prompt LLM with well-designed instructions to enable effective reasoning.

provided to specify the path that a UAV should follow. To achieve the navigation goal, the UAV considers both the instruction and visual perceptions, and predicts an action from the action space (right, left, up, down, forward, backward) with corresponding parameters at each time step  $t$ . Navigation ends when the UAV predicts a '*Stop*' action or reaches a pre-defined maximum action number. The navigation is recognized as a success if the UAV stops at a location that is less than 20 meters from the target location.

### B. Semantic-Topo-Metric Representation (STMR)

Previous LLM-based VLN methods use natural language to describe current observations, or nodes and edges of a topological graph to model the spatial information of the environment. However, in open scenarios, simple directional words such as "next to" or "aside" are not enough to describe complex spatial relationships, which can easily introduce ambiguity into LLMs. To address this challenge, we introduce the Semantic-Topo-Metric Representation (STMR) to enhance the spatial-aware reasoning capability of LLMs. Specifically, STMR incrementally takes an RGB image  $I_t^R$  and a depth map  $I_t^D$  as input from each step, and generates a dynamically updated matrix representation with semantic, topological, and metric information as its output. The details of STMR are presented as follows.

*a) 2D Visual Perception:* Impressed by the powerful open-vocabulary detection capabilities of Grounding DINO  $GD(\cdot)$ , as well as the captioning and segmentation capabilities of Tokenize Anything model  $TA(\cdot)$ , we integrate these two models as our 2D visual perceptor, as illustrated in Fig. 3. Given a single RGB image  $I_t^R$  and an instruction  $L$  as input, we first obtain detailed landmark categories using a Landmark Extractor  $LE(\cdot)$  driven by an LLM, and then identify the corresponding bounding box for each category through  $GD(\cdot)$ . Next, we employ  $TA(\cdot)$  to take each bounding box as a prompt and output a set of 2D semantic masks  $m^{(t)}$  and captions  $z^{(t)}$  for the current RGB image  $I_t^R$ . The entire process can be described as:

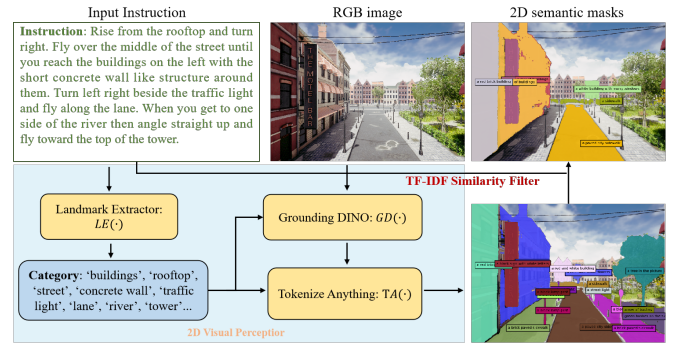


Fig. 3: 2D Visual Perceptor for the UAV.

$$\{m^{(t)}, z^{(t)}\} = TA(I_t^R, GD(I_t^R, LE(L))). \quad (1)$$

To improve the simplicity of the semantic masks and reduce the misleading of LLM-reasoning caused by numerous open-vocabulary categories, we propose a text-matching method to mitigate over-classification. As shown in Fig. 3, our method involves vectorizing the landmarks extracted from the instruction and the captions  $z^{(t)}$  generated in each  $I_t^R$ . Then, we calculate the cosine similarity between these vectorized landmarks and captions using TF-IDF [36]. If the similarity score exceeds the threshold  $\tau > 0.8$ , the landmark is classified as visible in the current view. By implementing this strategy, we effectively simplify semantic masks and ensure the LLM's reasoning focuses on relevant categories.

*b) Sub-goal-driven top-down map:* Considering that the top-down view can better express spatial relationships than the first-person view, we further utilize the depth image  $I_t^D$  to map semantic masks to 3D space, and then convert them into a top-down map. Specifically, with the RGB image  $I_t^R$  processed by the 2D visual perceptor, we produce first-person view predictions by assigning semantic labels to each pixel, resulting in a segmented image with identified objects and regions. Subsequently, the depth image  $I_t^D$  is converted into a 3D point cloud, where each pixel is mapped to a 3D point  $(X, Y, Z)$  based on its depth value and camera parameters:

$$X = \frac{(u - c_x)I_t^D(u, v)}{f_x}, Y = \frac{(v - c_y)I_t^D(u, v)}{f_y}, Z = I_t^D(u, v), \quad (2)$$

where  $(u, v)$  are the pixel coordinates,  $(c_x, c_y)$  are the camera's principal point coordinates, and  $(f_x, f_y)$  are the focal lengths. The semantic labels from the segmented RGB image are mapped to the corresponding 3D point clouds, resulting in a point cloud with semantic information  $(X, Y, Z, C_i)$ , where  $C_i$  are the semantic categories. Then the 3D point cloud is partitioned into discrete voxels, where each voxel aggregates its point clouds as one semantic category using max pooling described in [37]. Considering that UAVs usually fly above ground objects, for a specific coordinate  $(x, y)$ , the semantic label of the top one in a column of voxels will be projected into the top-down map:

$$\text{TopDownMap}(x, y) = \text{Voxel}(x, y, z_{top}), \quad (3)$$

where  $z_{top}$  means the highest  $z$  coordinate at location  $(x, y)$  and  $\text{Voxel}(x, y, z_{top})$  denotes the corresponding semantic label. So, we get a top-down map with semantic information.

Notably, since the LLM prioritizes the landmarks in the current sub-goal, if a category contained in the sub-goal appears in the voxel at any  $z$  coordinate, this category will be projected into the top-down map first. Thus we can modify Eq. (3) as:

$$\text{TopDownMap}(x, y) = \begin{cases} C_i, & C_i \text{ in sub-goal} \\ \text{Voxel}(x, y, z_{top}), & \text{otherwise.} \end{cases} \quad (4)$$

At each step, the position of a UAV will also be recorded as waypoints with special values and projected onto the top-down map.

*c) Matrix representation:* We found that directly inputting the image-format top-down map to a vision-language model (VLM) often yields poor reasoning results. Therefore, we process the visual map into a text-based matrix representation, which is input to an LLM to guide the navigation. Specifically, the UAV incrementally collects observations and gradually constructs the sub-goal-driven top-down map of the surrounding environment. Considering the perception quality of onboard sensors and the effective processing capacity of modern LLMs, we define a local map centered at the UAV's current position as shown in Fig. 1. Subsequently, we generate a matrix by partitioning the local map into a  $20 \times 20$  coordinate grid and applying semantic max pooling in each grid, making them finally contain one semantic category. Particularly, we grade all values that fall in each grid in the local map according to frequency, showing only the most frequent features as the final category of this grid. Each category such as buildings or cars are discriminated by different number labels. Furthermore, the distance between each grid, denoted as  $r$  (5m), is also input to the LLM as the metric information. In this case, the LLM can directly reason about positional relationships among each landmark.

### C. Designing Text Prompt for LLM Planning

Given that LLMs are well-trained in reasoning and planning, we complement their spatial perception and scene understanding capability with formatted prompt and action space. This prompt involves two components. First, the task description is prepared which includes the definition of the environment and the UAV, as well as the format of input and output. We require an LLM to leverage Chain-of-Thought reasoning [38] after capturing the observation, thinking step by step in an order of observation-thought-planning-history to predict the next action. Regarding the input instruction, sub-goals are extracted by the LLM, and the landmarks given in the instructions will be updated in the task definition as the scene changes. Second, to improve the quality of prompts, we implemented a cyclic refinement process. This involves designing a new set of instructions for an LLM, including elements such as 'history action' and 'next planning' corresponding to the STMR module. The task description also emphasizes updating the status of

planning, including three states, *i.e.*, *todo*, *in process*, and *completed*. The STMR is gradually updated in this iterative process as the UAV explores to improve the accuracy and relevance of the prompts.

### Example of LLM Prompt

**[Task Description]** You are an embodied unmanned aerial vehicle that navigates in the real world. You need to explore between some places marked and ultimately find the destination to stop.

**[Input Format]:** **‘Instruction’** is a global, step-by-step detailed guidance. **‘History’** is your previously executed actions. **‘Map’** is a top-down coordinate map, using a  $20 \times 20$  matrix  $M$  to represent coordinates. The numbers in the matrix represent different landmarks. You are at [10,10] of the matrix, which is a special value denoting your orientation, *e.g.*, west0 means face due west and the declination angle is 0 degree. The distance between adjacent numbers is 5 meters in the real world. The numbers in the matrix  $M$  represent:

[0:Unexplored 1:road 2:building ... -1:your past trajectory]. **‘Plan’** records previous long-term multi-step planning info that you can refer to now.

**[Output Format]** **‘Thought’**: your thoughts about the task, which may include your comprehension, surroundings, history, and *etc.* **‘Observation’**: the description of the map. **‘Plan’**: your updated plan. **‘Action’**: your next action." Think step by step. First, judge by the ‘Map’, give a first ‘Thought’, and depict your orientation. Second, check that if a landmark in the current ‘plan’ is within 5 meters of your current position, then based on ‘Instruction’ and the previous ‘Plan’, update your multi-step ‘Plan’. Each plan needs to follow a state word (TODO, In Process, Completed). Finally, judge by the ‘Map’ again, and give the specific "Action" according to the action format. Action format: Action: (right, left, lift, down, straight, back), (degree (0-15 degrees)), (distance (0-10 meters)).

**Instruction:** lift off and head straight across the water to the road...

**History:** [lift off 5 meters...]

**Map:** STMR

**Plan:**

1. (Completed) Lift off 5 meters.
2. (Completed) Turn 180 degrees.
3. (Completed) Head straight across the water to the road.
4. (In Process) Turn left to align the road.
5. (TODO)...

## IV. EXPERIMENT SETUP

*a) Datasets:* We conduct experiments using a novel and complex dataset provided by [1], which we refer to as the "AerialVNL-S" dataset, to assess the performance of aerial VLN tasks. This dataset is designed to mimic real-world urban environments with more than 870 different kinds of objects and various scenarios including downtown cities, factories, parks, and villages. Besides, the AerialVNL-S dataset encompasses 8,446 flying paths recorded by experienced human UAV pilots who possess the AOPA (Aircraft Owners and Pilots Association) certificate, ensuring the paths' realism and quality. Several comparison methods are evaluated on this dataset, including state-of-the-art VLN models, to

TABLE I: Comparison on the validation seen and unseen set of the AerialVNL-S dataset.

#	AerialVNL-S	Validation Seen			Validation Unseen		
		NE/m ↓	SR/% ↑	OSR/% ↑	NE/m ↓	SR/% ↑	OSR/% ↑
S1	Random	109.6	0.0	0.0	149.7	0.0	0.0
S2	Action Sampling	213.8	0.9	5.7	237.6	0.2	1.1
S3	LingUNet [25]	383.8	0.6	6.9	368.4	0.4	3.6
S4	Seq2Seq [13]	146.0	4.8	19.8	218.9	2.3	11.7
S5	CMA [1]	121.0	3.0	23.2	172.1	3.2	16.0
S6	LAG [1]	<b>90.2</b>	7.2	15.7	127.9	5.1	10.5
S7	<b>Ours</b>	96.3	<b>12.6</b>	<b>31.6</b>	<b>119.5</b>	<b>10.8</b>	<b>23.0</b>

establish a benchmark for aerial VLN tasks. We utilize AerialVNL-S as the benchmark, with 12 scenes from the validation seen set and 5 scenes from the validation unseen set, respectively. Notably, the test set is not used because it is inaccessible and the evaluation server [1] is unavailable now.

*b) Evaluation metrics:* To rigorously assess the performance of our method, we utilize a comprehensive set of evaluation metrics as in [1]. We focus on several key aspects, *i.e.*, Navigation Error (NE) quantifying the distance between the UAV’s stopping point and the actual destination, Success Rate (SR) which measures the proportion of navigations that successfully reach the destination within a 20-meter threshold, and Oracle Success Rate (OSR), an idealized measure considering any point on the trajectory that comes within 20 meters of the destination as a success.

*c) Implementation details:* Our framework is implemented in both a simulator and a real environment. For the simulation environment, we evaluated the algorithm on airsim and UE4, on a laptop with an Intel i9 12th generation CPU and an Nvidia RTX 4090 GPU. For the outdoor environment, we test on a Q250 airframe, carrying an Intel RealSense D435i depth camera, and an NVIDIA Jetson Xavier NX running Ubuntu 18.04 as onboard computer. We use the online API of GPT-4V and GPT-4o, where the default parameters are employed.

### A. Experimental Results

*a) Quantitative results in simulator:* Table I compares our method with several other works. Random and Action Sampling respectively mean sampling actions randomly and according to the action distribution of the training set. LingUNet [25] assumes an agent can see the destination from the beginning, which is transformed into a step-wise paradigm by [1]. Seq2Seq [13] is a learning-based recurrent policy, directly predicting the next action. CMA is a baseline model in [1], considering attention between multi-modalities. LAG is the main method in [1], designing a look-ahead guidance to adjust paths. In comparison, our method significantly outperforms others in most metrics, demonstrating the superiority of our method. We found that instead of processing the entire long instruction and visual observations at each time step, the formatted decomposed sub-goal is more conducive to the fine-grained alignment of each action and

TABLE II: Qualitative results in real environment.

Module	SR/%↑	OSR/%↑
MapGPT [10]	20	20
NavGPT [6]	10	20
<b>Ours</b>	<b>40</b>	<b>70</b>

landmark. Moreover, UAV has a better understanding of its own spatial position and other semantic constraints under the guidance of our STMR, which has obvious advantages in long instruction environments and leads to more robust execution.

*b) Quantitative results in real environment:* To test whether our solution works well in the real world, we collect 10 outdoor scenes including street scenes and forests with ground-truth lengths ranging from 50m to 500m. Then, we apply our method on real UAVs and call cloud-hosted LLMs (GPT-4o is used) to navigate in these challenging environments. LLM-based VLN methods MapGPT [10] and NavGPT [6] are employed and compared in this experiment. From demo snapshot Fig. 4, we can see that our method can align visual and textual landmarks as well as understand commands. Finally, the UAV reaches the destination successfully. Table II also shows that the proposed method achieves much better results than most recent LLM-based VLN methods.

*c) Failure case analysis:* In the simulation, we analyze two most common failures caused by incorrect planning or execution. The first typical failure is the misunderstanding of ambiguous instructions. In some instructions, there are a lot of continuous commands without any landmark, such as “turn left, then move right, then go straight”, which have no objects for an LLM to refer to. This case will directly leads to the repeated execution of a step. The second typical error is caused by the inaccuracy of the visual perceptor. Although modern perception models show strong ability, they still need to be improved in identifying objects from different views. As a result, the key landmark may not be mapped to the matrix representation, causing the proper action not to be completed. This observation aligns with our real-world experiment, where most errors are from perceptions.

### B. Comprehensive Analysis

We carry out several ablation studies to assess the effectiveness of the proposed framework. All ablation experiments are conducted on the AerialVNL-S task with the validation

Instruction: Go along the **road** and slightly turn right in front of the **trees**, fly across the **bridge**, turn right beside the **car** and go forward, stop next to the **building**.

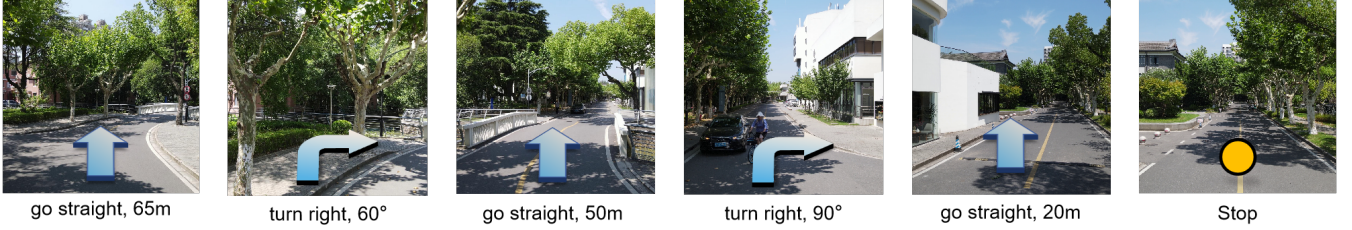


Fig. 4: Qualitative results in real environment. Short-range movements of the same action are merged into a single long-range movement, as shown in the images sequence.

TABLE III: Ablation study on randomly selected 100 scenes from Validation Unseen dataset for different semantic spatial representations as prompts.

#	Method	Validation Unseen		
		NE/m ↓	SR/% ↑	OSR/% ↑
1	Topo	203.3	4.9	12.8
2	Metric	165.0	6.1	13.7
3	Ours	<b>87.1</b>	<b>19.4</b>	<b>26.2</b>

unseen dataset. Corresponding results are depicted in [Table III](#), [Table IV](#) and [Table V](#).

*a) Explicit spatial information:* To demonstrate the spatial representation ability of STMR, we further compare it with other prompting formats as an LLM's spatial information prompt. In Topo format (row 1 of [Table III](#), we maintain a linguistic-formed map that captures the topological relationships between different nodes. Each node records textual descriptions of visual observations, and the connectivity between nodes is described using textual prompts. For example, "Place 1 is connected with Places 2, 4, 0, 3". In Metric format (row 2 of [Table III](#), we arrange the visual observations from 8 different directions in a clockwise order relative to the agent's current orientation and concatenate them into a single prompt. Each vision observation records the direction and distance of the landmark, for example, "a white building in the left front 10 meters away". It is shown that row 2 improves SR by 1.2% (absolute) over row 1 but still poorer navigation performance, since for some landmarks such as roads and rivers, UAVs still cannot obtain region-level spatial information based on a certain point distance description. Our STMR combining the semantic, topological, and metric information significantly enhances the UAV's exploration capability and improves the accuracy in SR and OSR by over 10%.

*b) State update of sub-goal:* To ensure that each sub-goal will be executed despite environment changes, in each iteration, the LLM does not change the original path plan, but updates the status of the current sub-goal according to the observation, including *todo*, *in process*, and *completed*. We compare this strategy with updating the entire multi-step path planning (row 1) according to the observation in each iteration. The results are shown in [Table IV](#). This strategy does not notably enhance the Oracle Success Rate (OSR), showing that the proposed STMR already furnishes enough

TABLE IV: Ablation study for the state update.

Module	NE/m↓	SR/%↑	OSR/%↑
w/o state	289.7	9.0	22.1
w state	<b>219.8</b>	<b>10.8</b>	<b>23.0</b>

TABLE V: Ablation study for the direct use of RGB images and the proposed STMR as the visual prompt for LLMs.

Input LLM \	RGB	STMR	NE/m↓	SR/%↑	OSR/%↑
GPT-4V	✓	✓	350.0 193.1	1.5 5.6	9.7 17.4
GPT-4o	✓	✓	412.0 119.5	1.1 10.8	10.0 23.0

capacity for navigating the environment comprehensively. Nonetheless, it positively impacts the decision-making process, resulting in an increase in the success rate (SR) from 9.0% to 10.8%.

*c) Direct visual input and STMR:* Due to the strong multi-modal capabilities of GPT-4V and GPT-4o, they can reason with both visual and textual prompts. However, it is challenging for them to understand landmark semantics directly from step-by-step input RGB images. This may be because the inability of LLMs in spatial-aware reasoning. As shown in [Table V](#), the proposed STMR representation with LLMs significantly outperforms the direct input of RGB images with VLMs.

## V. CONCLUSIONS AND FUTURE WORK

This paper addresses the challenging aerial VLN task by introducing an LLM-based end-to-end framework. To enhance the spatial reasoning ability of LLMs, we propose Semantic-Topo-Metric Representation (STMR). STMR first integrates instruction-related landmarks and their locations into a top-down map, and subsequently transforms this map into a matrix representation containing semantic, topological, and distance metric information. Taking the proposed STMR as a part of prompts of the LLM, we significantly improve the UAV's navigation capabilities. Our framework achieves state-of-the-art results on the AerialVLN-S dataset, demonstrating its effectiveness. In the future, we will explore flexible framework that will interact with humans to eliminate ambiguities in the instructions.

## REFERENCES

[1] S. Liu, H. Zhang, Y. Qi, P. Wang, Y. Zhang, and Q. Wu, “Aerialvln: Vision-and-language navigation for uavs,” in *International Conference on Computer Vision (ICCV)*, 2023.

[2] M. Ahn, A. Brohan, N. Brown, Y. Chebotar, O. Cortes, B. David, C. Finn, K. Gopalakrishnan, K. Hausman, A. Herzog, *et al.*, “Do as I can, not as I say: Grounding language in robotic affordances,” *arXiv preprint arXiv:2204.01691*, 2022.

[3] C. H. Song, J. Wu, C. Washington, B. M. Sadler, W.-L. Chao, and Y. Su, “Llm-planner: Few-shot grounded planning for embodied agents with large language models,” in *Proceedings of the IEEE/CVF International Conference on Computer Vision*, 2023, pp. 2998–3009.

[4] D. Driess, F. Xia, M. S. Sajjadi, C. Lynch, A. Chowdhery, B. Ichter, A. Wahid, J. Tompson, Q. Vuong, T. Yu, *et al.*, “Palm-e: An embodied multimodal language model,” *arXiv preprint arXiv:2303.03378*, 2023.

[5] W. Huang, F. Xia, T. Xiao, H. Chan, J. Liang, P. Florence, A. Zeng, J. Tompson, I. Mordatch, Y. Chebotar, P. Sermanet, T. Jackson, N. Brown, L. Luu, S. Levine, K. Hausman, and B. Ichter, “Inner monologue: Embodied reasoning through planning with language models,” in *6th Annual Conference on Robot Learning*, 2022. [Online]. Available: <https://openreview.net/forum?id=3R3Pz5i0tye>

[6] G. Zhou, Y. Hong, and Q. Wu, “Navgpt: Explicit reasoning in vision-and-language navigation with large language models,” in *Proceedings of the AAAI Conference on Artificial Intelligence*, vol. 38, no. 7, 2024, pp. 7641–7649.

[7] D. Shah, B. Osinski, S. Levine, *et al.*, “Lm-nav: Robotic navigation with large pre-trained models of language, vision, and action,” in *Conference on robot learning*. PMLR, 2023, pp. 492–504.

[8] D. Li, W. Chen, and X. Lin, “Tina: Think, interaction, and action framework for zero-shot vision language navigation,” *arXiv preprint arXiv:2403.08833*, 2024.

[9] B. Lin, Y. Nie, Z. Wei, J. Chen, S. Ma, J. Han, H. Xu, X. Chang, and X. Liang, “Navcot: Boosting llm-based vision-and-language navigation via learning disentangled reasoning,” *arXiv preprint arXiv:2403.07376*, 2024.

[10] J. Chen, B. Lin, R. Xu, Z. Chai, X. Liang, and K.-Y. K. Wong, “Mapgpt: Map-guided prompting for unified vision-and-language navigation,” *arXiv preprint arXiv:2401.07314*, 2024.

[11] S. Liu, Z. Zeng, T. Ren, F. Li, H. Zhang, J. Yang, C. Li, J. Yang, H. Su, J. Zhu, *et al.*, “Grounding dino: Marrying dino with grounded pre-training for open-set object detection,” *arXiv preprint arXiv:2303.05499*, 2023.

[12] T. Pan, L. Tang, X. Wang, and S. Shan, “Tokenize anything via prompting,” *arXiv preprint arXiv:2312.09128*, 2023.

[13] P. Anderson, Q. Wu, D. Teney, J. Bruce, M. Johnson, N. Sünderhauf, I. Reid, S. Gould, and A. Van Den Hengel, “Vision-and-language navigation: Interpreting visually-grounded navigation instructions in real environments,” in *Proceedings of the IEEE conference on computer vision and pattern recognition*, 2018, pp. 3674–3683.

[14] D. Fried, R. Hu, V. Cirik, A. Rohrbach, J. Andreas, L.-P. Morency, T. Berg-Kirkpatrick, K. Saenko, D. Klein, and T. Darrell, “Speaker-follower models for vision-and-language navigation,” *Advances in neural information processing systems*, vol. 31, 2018.

[15] Y. Qi, Z. Pan, S. Zhang, A. van den Hengel, and Q. Wu, “Object-and-action aware model for visual language navigation,” in *European Conference on Computer Vision*. Springer, 2020, pp. 303–317.

[16] Y. Hong, C. Rodriguez, Y. Qi, Q. Wu, and S. Gould, “Language and visual entity relationship graph for agent navigation,” *Advances in Neural Information Processing Systems*, vol. 33, pp. 7685–7696, 2020.

[17] D. An, Y. Qi, Y. Huang, Q. Wu, L. Wang, and T. Tan, “Neighbor-view enhanced model for vision and language navigation,” in *Proceedings of the 29th ACM International Conference on Multimedia*, 2021, pp. 5101–5109.

[18] X. Wang, W. Xiong, H. Wang, and W. Y. Wang, “Look before you leap: Bridging model-free and model-based reinforcement learning for planned-ahead vision-and-language navigation,” in *Proceedings of the European Conference on Computer Vision (ECCV)*, 2018, pp. 37–53.

[19] H. Tan, L. Yu, and M. Bansal, “Learning to navigate unseen environments: Back translation with environmental dropout,” *arXiv preprint arXiv:1904.04195*, 2019.

[20] H. Wang, Q. Wu, and C. Shen, “Soft expert reward learning for vision-and-language navigation,” in *Computer Vision–ECCV 2020: 16th European Conference, Glasgow, UK, August 23–28, 2020, Proceedings, Part IX 16*. Springer, 2020, pp. 126–141.

[21] W. Hao, C. Li, X. Li, L. Carin, and J. Gao, “Towards learning a generic agent for vision-and-language navigation via pre-training,” in *Proceedings of the IEEE/CVF conference on computer vision and pattern recognition*, 2020, pp. 13137–13146.

[22] A. Majumdar, A. Shrivastava, S. Lee, P. Anderson, D. Parikh, and D. Batra, “Improving vision-and-language navigation with image-text pairs from the web,” in *Computer Vision–ECCV 2020: 16th European Conference, Glasgow, UK, August 23–28, 2020, Proceedings, Part VI 16*. Springer, 2020, pp. 259–274.

[23] V. Blukis, N. Brukhim, A. Bennett, R. A. Knepper, and Y. Artzi, “Following high-level navigation instructions on a simulated quadcopter with imitation learning,” *arXiv preprint arXiv:1806.00047*, 2018.

[24] V. Blukis, D. Misra, R. A. Knepper, and Y. Artzi, “Mapping navigation instructions to continuous control actions with position-visitation prediction,” in *Conference on Robot Learning*. PMLR, 2018, pp. 505–518.

[25] D. Misra, A. Bennett, V. Blukis, E. Niklasson, M. Shatkhin, and Y. Artzi, “Mapping instructions to actions in 3d environments with visual goal prediction,” *arXiv preprint arXiv:1809.00786*, 2018.

[26] W. Huang, C. Wang, R. Zhang, Y. Li, J. Wu, and L. Fei-Fei, “Voxposer: Composable 3d value maps for robotic manipulation with language models,” *arXiv preprint arXiv:2307.05973*, 2023.

[27] W. Yu, N. Gileadi, C. Fu, S. Kirmani, K.-H. Lee, M. G. Arenas, H.-T. L. Chiang, T. Erez, L. Hasenclever, J. Humplik, *et al.*, “Language to rewards for robotic skill synthesis,” *arXiv preprint arXiv:2306.08647*, 2023.

[28] V. S. Dombala, G. Sigurdsson, R. Piramuthu, J. Thomason, and G. S. Sukhatme, “Clip-nav: Using clip for zero-shot vision-and-language navigation,” *arXiv preprint arXiv:2211.16649*, 2022.

[29] B. Chen, F. Xia, B. Ichter, K. Rao, K. Gopalakrishnan, M. S. Ryoo, A. Stone, and D. Kappler, “Open-vocabulary queryable scene representations for real world planning,” in *2023 IEEE International Conference on Robotics and Automation (ICRA)*. IEEE, 2023, pp. 11509–11522.

[30] Y. Cui, S. Niekum, A. Gupta, V. Kumar, and A. Rajeswaran, “Can foundation models perform zero-shot task specification for robot manipulation?” in *Learning for dynamics and control conference*. PMLR, 2022, pp. 893–905.

[31] M. Shridhar, L. Manuelli, and D. Fox, “Cliport: What and where pathways for robotic manipulation,” in *Conference on robot learning*. PMLR, 2022, pp. 894–906.

[32] I. Singh, V. Blukis, A. Mousavian, A. Goyal, D. Xu, J. Tremblay, D. Fox, J. Thomason, and A. Garg, “Progprompt: Generating situated robot task plans using large language models,” in *2023 IEEE International Conference on Robotics and Automation (ICRA)*. IEEE, 2023, pp. 11523–11530.

[33] J. Wu, R. Antonova, A. Kan, M. Lepert, A. Zeng, S. Song, J. Bohg, S. Rusinkiewicz, and T. Funkhouser, “Tidybot: Personalized robot assistance with large language models,” *arXiv preprint arXiv:2305.05658*, 2023.

[34] J. Liang, W. Huang, F. Xia, P. Xu, K. Hausman, B. Ichter, P. Florence, and A. Zeng, “Code as policies: Language model programs for embodied control,” in *2023 IEEE International Conference on Robotics and Automation (ICRA)*. IEEE, 2023, pp. 9493–9500.

[35] A. Zeng, M. Attarian, B. Ichter, K. Choromanski, A. Wong, S. Welker, F. Tombari, A. Purohit, M. Ryoo, V. Sindhwani, J. Lee, V. Vanhoucke, and P. Florence, “Socratic models: Composing zero-shot multimodal reasoning with language,” *arXiv preprint arXiv:2204.00598*, 2022.

[36] S. Qaiser and R. Ali, “Text mining: use of tf-idf to examine the relevance of words to documents,” *International Journal of Computer Applications*, vol. 181, no. 1, pp. 25–29, 2018.

[37] D. S. Chaplot, D. Gandhi, S. Gupta, A. Gupta, and R. Salakhutdinov, “Learning to explore using active neural slam,” *arXiv preprint arXiv:2004.05155*, 2020.

[38] J. Wei, X. Wang, D. Schuurmans, M. Bosma, B. Ichter, F. Xia, E. Chi, Q. Le, and D. Zhou, “Chain of thought prompting elicits reasoning in large language models,” *arXiv preprint arXiv:2201.11903*, 2022.